Desalination and Water Treatment
www.deswater.com
doi: 10.5004/dwt.2019.24672

169 (2019) 363–371
November

Decolorization of reactive azo dye from aqueous solutions with Fenton oxidation process: effect of system parameters and kinetic study

Nejdet Değermenci*, Gökçe Didar Değermenci, Hatice Bike Ulu

Department of Environmental Engineering, Kastamonu University, Kastamonu 37200, Turkey, emails: ndegermenci@gmail.com/degermenci@kastamonu.edu.tr (N. Değermenci)

Received 11 February 2019; Accepted 8 July 2019

ABSTRACT

The decolorization of Drimaren Orange HF 2GL (DOHF) reactive azo dye from aqueous solutions with the Fenton oxidation process was researched. With the aim of determining optimum conditions, the effects of different operating parameters such as H_2O_2, Fe(II), chloride ion and initial DOHF concentration, initial pH and solution temperature on the decolorization were investigated. Optimum conditions were determined as 30°C temperature, pH 3, 300 mg/L DOHF, 15 mg/L Fe(II) and 100 mg/L H_2O_2. The presence of chloride ion had a negative effect on the decolorization, while the increase in reaction temperature caused an increase in the decolorization. Using experimental data, the decolorization kinetics for dye molecules was investigated and the best kinetic model representing experimental data was found to be the Behnajady–Modirshahla–Ghanbary (BMG) kinetic model. Additionally, Fourier transform infrared spectroscopy analysis was performed before and after Fenton oxidation to show degradation of dye molecules.

Keywords: Oxidation; Kinetics; Decolorization; IR spectroscopy

1. Introduction

The global environmental problem of water pollution, which is increasing daily, has become an important factor affecting human life and limiting social life. In proportion with the increase in requirements due to rapid industrialization, the use of coloring chemicals such as dyes has increased [1,2]. Dyes are substances used in the textile, paper, cosmetic, food and pharmaceutical industries which also have structural varieties that cause important environmental damage by polluting the receiving aquatic environment. Globally, approximately 700,000 tons of 10,000 dye and pigment types are produced yearly, and 20% of these dyes mix to wastewater during dyeing processes [3–5]. Synthetic dyes containing many aromatic rings are known to be very resistant to biological degradation. Due to being toxic, carcinogenic and mutagenic, these compounds form a threat to human health and ecosystems and must be removed from wastewater [6–8]. When wastewater containing synthetic dyes are discharged into the receiving environment without the use of appropriate treatment methods, photosynthesis of plants living in water is prevented due to the reduction in light transmission, causing anoxic conditions deadly for aquatic organisms due to depletion of dissolved oxygen, the esthetic appearance of the water is disrupted and possibilities to reuse water are limited [2,9,10]. A variety of physical, chemical and biological methods have been developed for removal from these wastewaters such as chemical precipitation, membrane filtration, adsorption, Fenton oxidation, ozonation and aerobic and/or anaerobic treatment [11]. Physicochemical methods for wastewater treatment are accepted as more expensive than biological treatment methods; however, biological treatment methods are insufficient

* Corresponding author.

to remove color-giving materials and other refractory compounds [12]. As a result, the use of advanced oxidation processes (AOPs) is unavoidable. The Fenton oxidation process is one of the most developed AOPs and is one of the simple and cheap treatment methods for wastewater containing dyes [13].

The oxidation mechanism in the environmentally friendly and easily operated Fenton oxidation process is based on production of hydroxyl radicals as a result of reactions between an Fe(II) catalyst and H_2O_2 under acidic conditions (Eq. (1)) [14]. Hydroxyl radicals are very reactive and non-selective oxidants that can oxidize organic material (oxidation potential 2.80 V) [15]. The Fenton oxidation process occurs in four stages including setting pH, oxidation, neutralization and coagulation [16]. In recent years, the Fenton oxidation process has been frequently used for removal of a variety of dyestuffs and pesticides [17,18].

$$Fe^{2+} + H_2O_2 + H^+ \rightarrow Fe^{3+} + OH^{\bullet} + H_2O \quad (1)$$

It is necessary to determine the optimum parameters in experimental conditions for the decolorization of DOHF with Fenton oxidation. In this study, the effects of a variety of operating parameters such as H_2O_2, Fe(II), initial DOHF, anion types and chloride ion concentration, pH and temperature on the decolorization of DOHF with Fenton oxidation were researched and the optimum decolorization conditions were determined. The fit of some kinetic models was tested using experimental data. Additionally, an attempt was made to determine the structural changes to the dye material with Fenton oxidation using FTIR analysis.

2. Material and methods

2.1. Chemicals

DOHF was obtained from a dye house in Kayseri (Turkey) and used without any purification procedures. Hydrogen peroxide (30%, w/w), iron sulfate hepta hydrate, sodium chloride, sodium nitrate, potassium sulfate, sulfuric acid and sodium hydroxide were obtained from Sigma-Aldrich (Germany). Solutions were all prepared using deionized water.

2.2. Experimental procedure

For the decolorization of DOHF with the Fenton oxidation process, one of the parameters affecting the decolorization was changed, while the others were held constant. The reactor used in the experiments was double-walled and operated in batch mode. For each experimental study, Fe(II) and DOHF were diluted to 500 mL with deionized water and then a pH meter (WTW, MultiLine Multi 3620 IDS, Germany) was used with 0.5 M H_2SO_4 and NaOH to set the pH to the desired value. Later H_2O_2 was added to the reactor to begin the reaction (reaction duration 1 h). Samples were periodically removed from the reactor with a pipette and immediately analyzed. During the reaction, a magnetic stirrer (IKA, RCT basic, Germany) was used to ensure homogeneity of the solution. Temperature was kept constant at the required temperature using a temperature-controlled heating-cooling circulator (LABO, C200-H13, Turkey).

2.3. Analytical methods

DOHF concentrations were determined using a UV–Vis spectrophotometer (Hach Lange, DR6000, Germany) by measuring absorbance values with a calibration curve prepared at maximum wavelength (416 nm). As the oxidation reaction continued during the Fenton process, absorbance measurements were completed immediately after obtaining the sample. The decolorization efficiency was calculated from the following equation;

$$\text{Decolorization efficiency},(\%) = \left(1 - \frac{C_t}{C_0}\right) \times 100 \quad (2)$$

where C_0 is the initial DOHF concentration and C_t is the DOHF concentration at time t.

After Fenton oxidation, structural changes in the dye were assessed using an infrared spectrophotometer (Bruker, Alpha, Germany) in the 500–4,000 cm^{-1} spectral interval (resolution 4 cm^{-1}, scans 24). At the end of the oxidation duration (60 min), the pH was set to 8.5 to stop the reaction. Later the solution was dried and FTIR analysis was performed on remaining solid residue.

3. Results and discussion

3.1. Effect of initial pH

The pH value of the solution is a parameter affecting the hydroxyl radical production rate, H_2O_2 and Fe(II) concentration in the Fenton oxidation process and one of the important operating parameters for wastewater treatment [19]. With the aim of finding the optimum pH value for the decolorization of DOHF with Fenton oxidation, a range of experiments with different initial pH values (2, 3, 4, 5, 6) were completed and the results obtained are shown in Fig. 1. During the reaction (60 min), no buffer was added to alter pH and experiments were completed with these initial pH values. The results show the solution pH significantly affects the decolorization of DOHF, with highest the decolorization efficiency of 87% obtained at pH 3 after 60 min. Many studies using Fenton oxidation emphasize the importance of solution pH, and reveal high oxidation ability under acidic conditions [14,20]. However, reactions occurring at low pH (pH < 3) may slow the decolorization because hydrogen peroxide may remain in balance by taking a proton to form oxonium ions ($H_3O_2^+$) (Eq. (3)) and hydrogen peroxide reduces reactivity of Fe(II) [21]. Additionally, H^+ ions in solution may cause scavenging of hydroxyl radicals (Eq. (4)) and reduce oxidation efficiency [22,23]. Another possibility is the complicated Fe(II) and Fe(III) species forming may enter slower reactions with hydrogen peroxide [24]. These reasons may explain the fall in the decolorization efficiency for DOHF at pH 2. However, in situations with pH > 4, there may be a reduction in hydroxyl radicals linked to hydrogen peroxide separating into water and oxygen (Eq. (5)) and formation of $Fe(OH)_3$ complexes (Eq. (6)) and oxidation efficiency may reduce [25,26]. Considering the decolorization efficiency, the optimum initial pH value was chosen as 3 and all later experiments were completed with this optimum initial pH value.

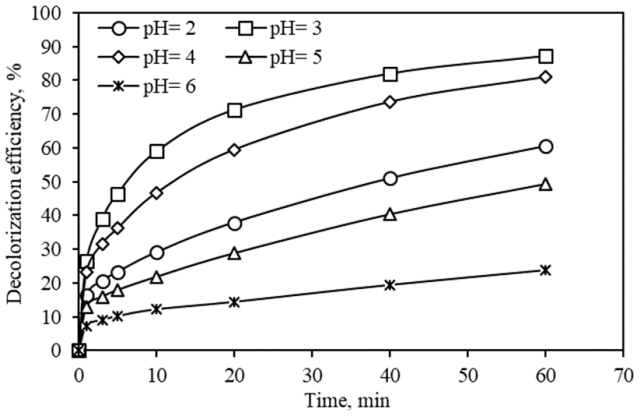

Fig. 1. Effect of pH on decolorization of DOHF with Fenton oxidation process $[Dye]_0$ = 200 mg/L, $[Fe(II)]_0$ = 10 mg/L, $[H_2O_2]_0$ = 200 mg/L and T = 20°C.

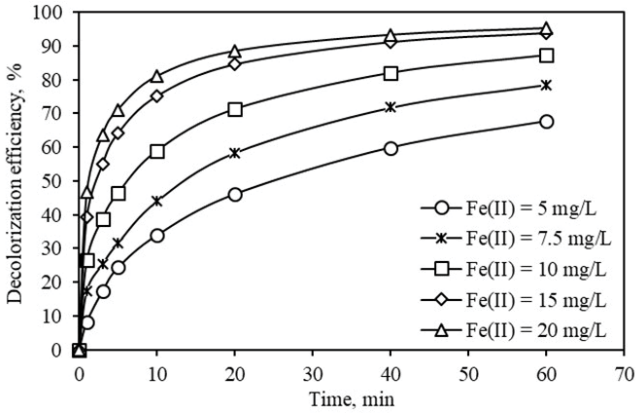

Fig. 2. Effect of Fe(II) on the decolorization of DOHF with Fenton oxidation process $[Dye]_0$ = 200 mg/L, pH = 3, $[H_2O_2]_0$ = 200 mg/L and T = 20°C.

$$H_2O_2 + H^+ \rightarrow H_3O_2^+ \quad (3)$$

$$^{\bullet}OH + H^+ + e^- \rightarrow H_2O \quad (4)$$

$$2H_2O_2 \rightarrow 2H_2O + O_2 \quad (5)$$

$$Fe^{3+} + 3OH^- \rightarrow Fe(OH)_3 \quad (6)$$

3.2. Effect of Fe(II) concentration

Fe(II) concentration is an important parameter in Fenton oxidation process. As a result, with the aim of determining the optimum Fe(II) concentration for the decolorization of DOHF, the initial DOHF concentration (200 mg/L), initial H_2O_2 concentration (200 mg/L), initial pH 3 and temperature (20°C) were kept fixed, while a range of experiments were completed with different Fe(II) concentrations (5, 7.5, 10, 15 and 20 mg/L). The effect of Fe(II) concentration on the decolorization is shown in Fig. 2. The results obtained showed that the decolorization was significantly linked to Fe(II). At 5 mg/L Fe(II) concentration, the decolorization was 34% at the end of 10 min reaction time, while it was 68% at the end of 60 min reaction time. At the end of 10 min reaction time, the increase in Fe(II) concentration of 7.5, 10, 15 and 20 mg/L Fe(II) led to the decolorization efficiency of 44%, 59%, 75% and 81%, respectively. The reason for this is that according to Eq. (1), there is more production of hydroxyl radicals with the increase in Fe(II) concentration. However, some studies have revealed that in situations with the use of Fe(II) at high concentrations, the reaction given in Eq. (7) is stimulated so hydroxyl radicals scavenge themselves and cause a fall in the removal rate of pollutants [27,28]. Additionally, increasing Fe(II) concentration is reported to cause an increase in dissolved solid matter content and turbidity [29,30]. Considering the results given in Fig. 2, for the decolorization of 200 mg/L DOHF the optimum Fe(II) concentration was selected as 15 mg/L.

$$^{\bullet}OH + Fe^{2+} \rightarrow Fe^{3+} + OH^- \quad (7)$$

3.3. Effect of H_2O_2 concentration

H_2O_2 concentration plays a very important role in determining the decolorization performance. Use at low amounts reduces the decolorization efficiency, while use at higher than necessary amounts increases residual H_2O_2 concentration interfere to chemical oxygen demand measurement and increasing treatment costs [31,32]. As a result, it is necessary to determine the optimum H_2O_2 concentration. With this aim, the initial DOHF concentration in the solution (200 mg/L), Fe(II) concentration (15 mg/L), initial pH (3) and temperature (20°C) were fixed with a range of experiments completed with different H_2O_2 concentrations (25, 50, 75, 100 and 200 mg/L). The results are shown in Fig. 3. The increase in H_2O_2 concentration from 25 to 200 mg/L increases the decolorization from 63.4% to 93.9%. In this situation, the increasing H_2O_2 concentration can explain the increase in the amount of hydroxyl radicals produced by the Fenton oxidation process (Eq. (1)) [1]. The use of high amounts of H_2O_2 will consume hydroxyl radicals (Eqs. (8)–(10)) and is stated to lower removal efficiency [28,33]. The optimum hydrogen peroxide concentration for 200 mg/L of dye is 100 mg/L with 90.4% the decolorization obtained.

$$H_2O_2 + {}^{\bullet}OH \rightarrow {}^{\bullet}HO_2 + H_2O \quad (8)$$

$$^{\bullet}OH + {}^{\bullet}HO_2 \rightarrow O_2 + H_2O \quad (9)$$

$$^{\bullet}OH + {}^{\bullet}OH \rightarrow \frac{1}{2}O_2 + H_2O \quad (10)$$

3.4. Effect of initial DOHF concentration

The concentration of the pollutant is an important factor in the Fenton oxidation process. As the concentration of pollutants found in wastewater may suddenly change, it is important to determine the effect of the pollutant concentration entering the treatment process on efficiency [34]. Fig. 4 shows the effect of initial DOHF concentration on the decolorization with the Fenton oxidation process. At the

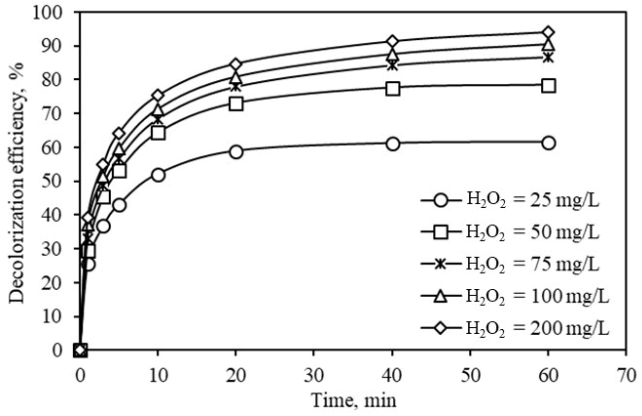

Fig. 3. Effect of H_2O_2 on the decolorization of DOHF with Fenton oxidation process $[Dye]_0$ = 200 mg/L, $[Fe(II)]_0$ = 15 mg/L, pH = 3 and T = 20°C.

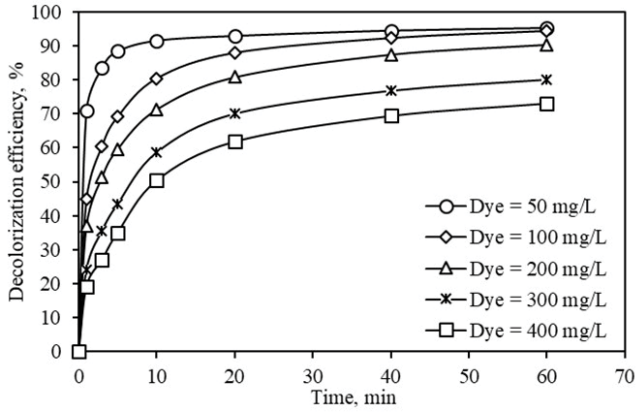

Fig. 4. Effect of dye concentration on the decolorization of DOHF with Fenton oxidation process $[Fe(II)]_0$ = 15 mg/L, $[H_2O_2]_0$ = 100 mg/L, pH = 3 and T = 20°C.

end of 60 min, 95.3% of 50 and 100 mg/L dye concentrations were removed, while the decolorization of 90.4%, 80.1% and 73.0% were obtained for 200, 300 and 400 mg/L dye concentrations. From these results, it is clearly understood that as the initial DOHF concentration increases, the decolorization efficiency reduces. The reason for this is that the other parameters (Fe(II) and H_2O_2) were fixed while the pollutant concentration increased [35]. In other words, as the hydroxyl radical concentration produced by fixed H_2O_2 and Fe(II) concentrations was the same, the decolorization reduced with the increase in dye concentration. At high pollutant (dye) concentrations, to ensure higher pollutant removal efficiency, it is necessary to increase the H_2O_2 and/or Fe(II) concentrations [36,37].

3.5. Effect of temperature

Temperature plays an important role in removal of pollutants with the Fenton oxidation process. With the aim of determining the effect of temperature on the decolorization, a range of experiments were completed at different temperatures (10°C, 20°C, 30°C, 40°C and 50°C). The results obtained are shown in Fig. 5, and it clearly shows that with the increase in temperature, the decolorization rate increased. The reason for this is that with the temperature increase, the reaction rate between H_2O_2 and Fe(II) increases and this forms higher amounts of hydroxyl radicals [36,38]. Additionally, the system may be operated at high temperatures to ensure the decolorization in a shorter period of time. Increasing the temperature from 10°C to 30°C increased the decolorization from 64.3% to 84.1% at the end of 60 min. At 40°C and 50°C, the decolorization was 85.6% and 87.1%, respectively. Based on these results, at the end of 60 min, the temperature increase after 30°C can be said not to affect the system performance significantly. Additionally, at high temperatures decomposition of hydrogen peroxide into water and oxygen (Eq. (5)) reduces the effective utilization [29].

3.6. Effect of anionic types

Wastewaters containing dye contains not only a particular target contaminant but considerable quantity of inorganic salts and ions [39]. There are many researches in the literature on how inorganic salts and ions affect the removal of different target contaminant [40,41]. Inorganic salts and ions contained in wastewater can reduce the removal of pollutant in the Fenton oxidation process. On the decolorization of dye in Fenton oxidation process, the effect of some common wastewater constituents such as chloride, nitrate and sulfate has been discussed in this section. As a result, initial pH 3, initial DOHF concentration 100 mg/L, H_2O_2 concentration 100 mg/L, temperature 20°C and Fe(II) concentration 15 mg/L were fixed and a range of experiments were completed with different inorganic anions (Fig. 6). Nitrate ions are insignificant for the Fenton oxidation process. The presence of sulfate ions affects the decolorization efficiency. The sulfate ion can attack the hydroxyl radical to produce less reactive oxidant (Eq. (11)). The increase in chloride ion concentration negatively affected the decolorization as can be seen in Fig. 6. At the end of 60 min, the decolorization is 94.8% when chloride ion is not added, but adding 0.15–0.60 g/L chloride ion reduces the decolorization efficiency from 92.5% to 82.2%. The reduction in

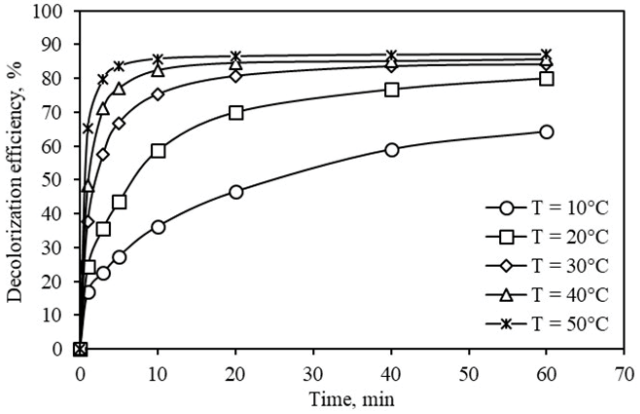

Fig. 5. Effect of temperature on the decolorization of DOHF with Fenton oxidation process $[Fe(II)]_0$ = 15 mg/L, $[H_2O_2]_0$ = 100 mg/L, pH = 3 and $[Dye]_0$ = 300 mg/L.

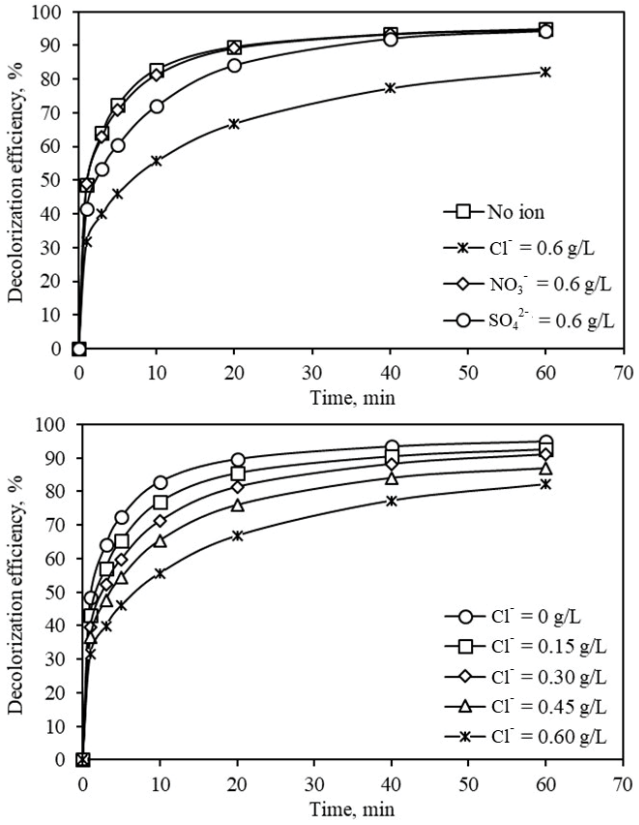

Fig. 6. Effect of anionic types and chloride ion concentration on the decolorization of DOHF with Fenton oxidation process $[Fe(II)]_0$ = 15 mg/L, $[H_2O_2]_0$ = 100 mg/L, pH = 3, T = 20°C and $[Dye]_0$ = 100 mg/L.

the decolorization with the addition of chloride ion can be explained by chloride ions forming less reactive radicals compared with hydroxyl radicals and scavenging hydroxyl radicals (Eqs. (12) and (13)) [42,43].

$$SO_4^{2-} + {}^{\bullet}OH \rightarrow SO_4^{\bullet-} + OH^- \quad (11)$$

$$Cl^- + {}^{\bullet}OH \rightarrow {}^{\bullet}ClOH^- \quad (12)$$

$${}^{\bullet}ClOH^- + Fe^{2+} \rightarrow Cl^- + OH^- + Fe^{3+} \quad (13)$$

3.7. Kinetic model for the decolorization

The kinetics of Fenton oxidation processes may be very complicated due to many reactions simultaneously occurring during the process [44]. The first-order, second-order and Behnajady–Modirshahla–Ghanbery (BMG) kinetic models were used to test the experimental data obtained for the decolorization of DOHF. The linear forms of these models are given in Eqs. (14)–(16) [19];

$$\ln C_t = \ln C_0 - k_1 t \quad (14)$$

$$\frac{1}{C_t} = \frac{1}{C_0} + k_2 t \quad (15)$$

$$\frac{t}{\left(1 - \frac{C_t}{C_0}\right)} = m + bt \quad (16)$$

where C_0 is initial DOHF concentration, C_t is DOHF concentration at time t, k_1 is first-order reaction rate constant and k_2 is second-order reaction rate constant. b and m represent two characteristic constants related to reaction kinetics and oxidation capacity in the BMG model. Under different reaction conditions, linear regression analysis was applied to calculate the kinetic model parameters for t against $\ln C_t$ for the first-order kinetic model, t against $1/C_t$ for the second-order kinetic model and t against $t/(1 - C_t/C_0)$ for the BMG kinetic model. The kinetic parameters obtained for the dye are given in Table 1.

The success of experimental data is determined according to the calculated determination coefficient (R^2) of regression analysis. If this coefficient is equal to 1 it proves the data fit perfectly with the linear curve. The results show the experimental data and the BMG kinetic model are more coherent. This kinetic model has been applied in different studies to define the decolorization kinetics of the Fenton process [19,45].

In the BMG kinetic model, the 1/m and 1/b constants show the initial DOHF removal rates and theoretical maximum of the decolorization fraction, respectively (Table 1). In the BMG kinetic model, the 1/m and 1/b constants may be associated with a variety of operating parameters such as pH, initial DOHF concentration, Fe(II) concentration, H_2O_2 concentration and temperature. The correlations between the pH, Fe(II) concentration, H_2O_2 concentration, initial DOHF concentration and temperature values for 1/m and 1/b values are given in Fig. 7. When the initial pH value of the dye solution is 3, the 1/m and 1/b reach maximum values as shown in Fig. 7a. Fig. 7b shows the variation in 1/m and 1/b values with the increase in Fe(II) concentration and it may be concluded the 1/m values increase linearly. With the increase in H_2O_2 concentration, the 1/b values can be said to increase linearly (Fig. 7c). With the increase in initial DOHF concentration, the variation in 1/m and 1/b values are shown in Fig. 7d with the 1/m values found to exponentially reduce. Fig. 7e shows the correlation between 1/m and 1/b values with temperature. With the temperature increase, the 1/m values exponentially increase. The correlations between pH, Fe(II) concentration, H_2O_2 concentration, initial DOHF concentration and temperature with 1/m and 1/b values can be expressed as mathematical equations. These correlations are given in Table 2.

3.8. FTIR analysis

FTIR spectra are commonly used for characterization of organic compounds in water or wastewater [46]. The FTIR spectra for the solid portion of DOHF and after the decolorization are given in Fig. 8. FTIR analysis was performed because the molecular structure of the dye was not found according to our literature review. When the FTIR spectrum is investigated, the peaks observed in a broad band from 3,600 to 3,000 cm^{-1} are O–H stretching vibrations, N–H stretching vibrations and intra-molecular and inter-molecular hydrogen bonds [47,48]. The peaks for $–CH_2$ stretching vibrations

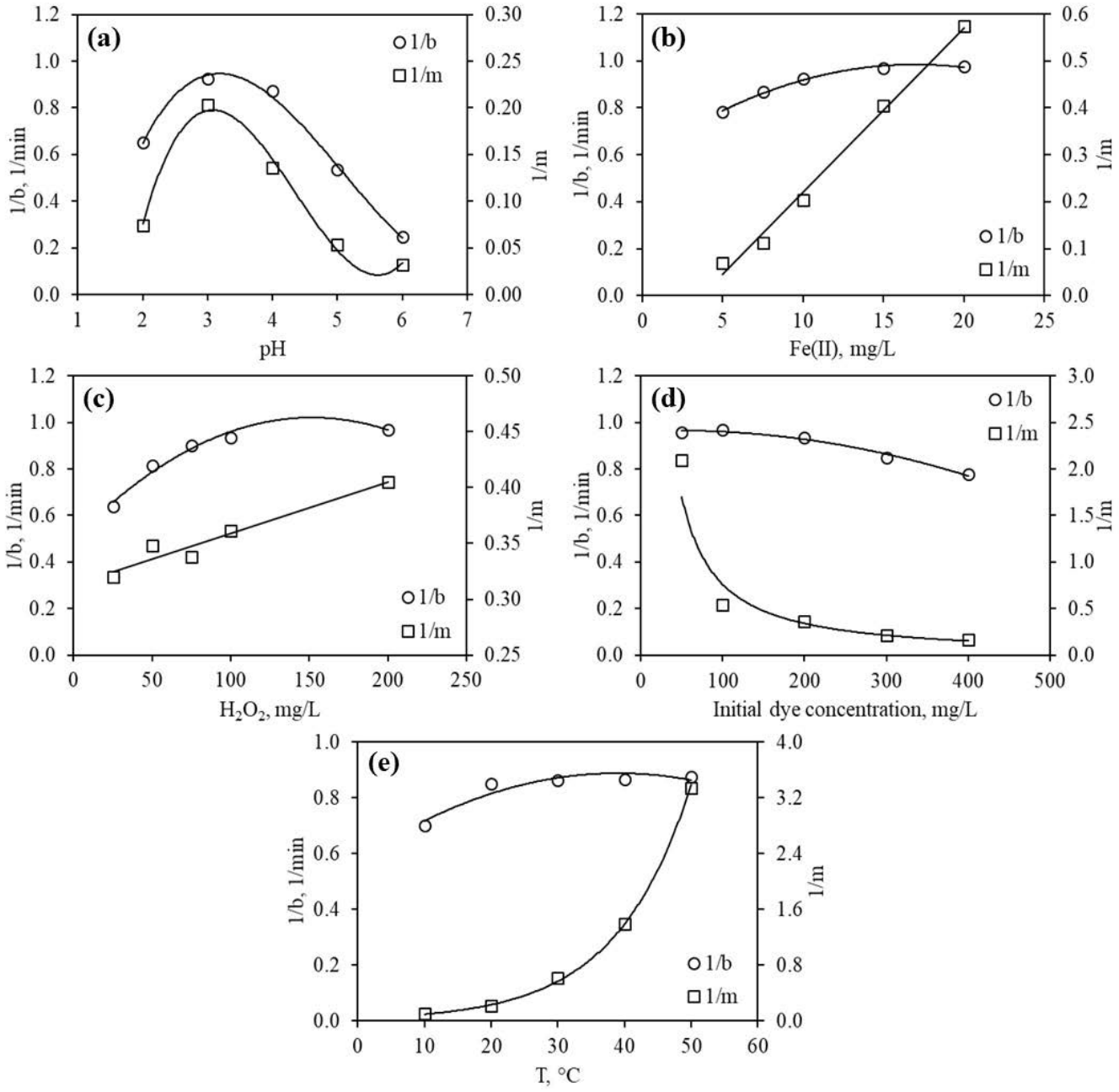

Fig. 7. Correlation of 1/*m* and 1/*b* values with (a) pH, (b) Fe(II), (c) H_2O_2, (d) initial dye concentration and (e) temperature.

are at 2,852 and 2,923 cm^{-1}, with bending vibrations observed in the interval 1,405–1,465 cm^{-1} [49]. Peaks at 1,572, 1,297 and 675 cm^{-1} are N=N, C–N and C–Cl stretching vibrations [50–52]. The peaks at 1,368 and 1,193 cm^{-1} show the presence of S=O stretching vibrations [53]. It is considered there are aromatic compounds, aromatic amines, alcohol compounds and azo compounds among the main organic pollutants contained in DOHF. The peaks at 1,097 and 615 cm^{-1} show the presence of sulfate ions and due to the added iron sulfate, the strength of these peaks increase [54,55]. After the decolorization of DOHF with the Fenton process, the intensity of the peaks (except 1,096 and 615 cm^{-1}) reduce and as a result it can be said the organic content is degraded.

4. Conclusions

Based on these experimental results, the decolorization of DOHF from aqueous solutions with the Fenton oxidation process was successfully completed. It was found that initial pH, H_2O_2 concentration, Fe(II) concentration, initial DOHF concentration, salt concentration and temperature had strong effects on the decolorization and these experimental parameters were optimized. Optimum conditions were determined as 30°C temperature, pH 3, 300 mg/L DOHF, 15 mg/L Fe(II) and 100 mg/L H_2O_2. The efficiency of DOHF the decolorization increased with the increase in reaction temperature; however, it was negatively affected by the increase in chloride

Table 1
Results of kinetic models calculated for the decolorization

pH	Fe(II)	H_2O_2	C_0	T	First order		Second order		BMG equation		
–	mg/L	mg/L	mg/L	°C	k_1	R^2	$k_2 \times 10^{-3}$	R^2	m	b	R^2
2	10	200	200	20	0.0135	0.9467	0.1142	0.9847	13.498	1.5301	0.9653
3	10	200	200	20	0.0311	0.9127	0.5464	0.9978	4.9222	1.0825	0.9970
4	10	200	200	20	0.0251	0.9443	0.3386	0.9963	7.3612	1.1477	0.9891
5	10	200	200	20	0.0098	0.9468	0.0730	0.9774	18.706	1.8703	0.9488
6	10	200	200	20	0.0036	0.8707	0.0211	0.8986	31.188	4.0255	0.9592
3	5	200	200	20	0.0180	0.9463	0.1674	0.9926	14.421	1.2767	0.9921
3	7.5	200	200	20	0.0241	0.9415	0.2938	0.9973	8.8974	1.1531	0.9914
3	10	200	200	20	0.0311	0.9127	0.5464	0.9978	4.9222	1.0825	0.9970
3	15	200	200	20	0.0411	0.8640	1.2148	0.9990	2.4688	1.0304	0.9995
3	20	200	200	20	0.0433	0.8241	1.5881	0.9972	1.7434	1.0256	0.9998
3	15	25	200	20	0.0122	0.6053	0.1162	0.6993	3.1282	1.5682	0.9997
3	15	50	200	20	0.0214	0.7074	0.2901	0.8433	2.8701	1.2262	0.9998
3	15	75	200	20	0.0291	0.8027	0.5317	0.9555	2.9579	1.1106	0.9995
3	15	100	200	20	0.0339	0.8376	0.7665	0.9867	2.7650	1.0683	0.9993
3	15	200	200	20	0.0411	0.8640	1.2148	0.9990	2.4688	1.0304	0.9995
3	15	100	50	20	0.0336	0.5223	5.9031	0.8517	0.4781	1.0437	1.0000
3	15	100	100	20	0.0411	0.8109	2.7106	0.9907	1.2865	1.0286	0.9999
3	15	100	200	20	0.0339	0.8376	0.7665	0.9867	2.7650	1.0683	0.9993
3	15	100	300	20	0.0243	0.8265	0.2229	0.9435	4.7147	1.1773	0.9989
3	15	100	400	20	0.0200	0.8392	0.1101	0.9341	6.1352	1.2885	0.9990
3	15	100	300	10	0.0156	0.9090	0.0968	0.9712	10.145	1.4253	0.9887
3	15	100	300	20	0.0243	0.8265	0.2229	0.9435	4.7147	1.1773	0.9989
3	15	100	300	30	0.0239	0.6182	0.2776	0.7932	1.6168	1.1606	1.0000
3	15	100	300	40	0.0214	0.4459	0.2706	0.6106	0.7203	1.1552	1.0000
3	15	100	300	50	0.0186	0.3204	0.2633	0.4688	0.2998	1.1423	1.0000

Table 2
Correlation equations for 1/m and 1/b values with pH, Fe(II) concentration, H_2O_2 concentration, initial DOHF concentration and temperature

Parameters	Equations	R^2
pH	$1/b = 0.031[\mathrm{pH}]^3 - 0.473[\mathrm{pH}]^2 + 2.065[\mathrm{pH}] - 1.838$	0.9958
	$1/m = 0.021[\mathrm{pH}]^3 - 0.280[\mathrm{pH}]^2 + 1.114[\mathrm{pH}] - 1.204$	0.9918
Fe(II)	$1/b = 0.0014[\mathrm{Fe(II)}]^2 - 0.0465[\mathrm{Fe(II)}] + 0.5901$	0.9932
	$1/m = 0.0351[\mathrm{Fe(II)}] - 0.1308$	0.9923
H_2O_2	$1/b = 0.000023[\mathrm{H_2O_2}]^2 - 0.0069[\mathrm{H_2O_2}] + 0.499$	0.9720
	$1/m = 0.00046[\mathrm{H_2O_2}] + 0.3132$	0.9338
Dye	$1/b = 0.0000015[\mathrm{Dye}]^2 - 0.00013[\mathrm{Dye}] + 0.963$	0.9840
	$1/m = 160.48[\mathrm{Dye}]^{-1.162}$	0.9582
T	$1/b = 0.0002[T]^2 - 0.0158[T] + 0.5795$	0.8970
	$1/m = 0.0392e^{0.0392[T]}$	0.9979

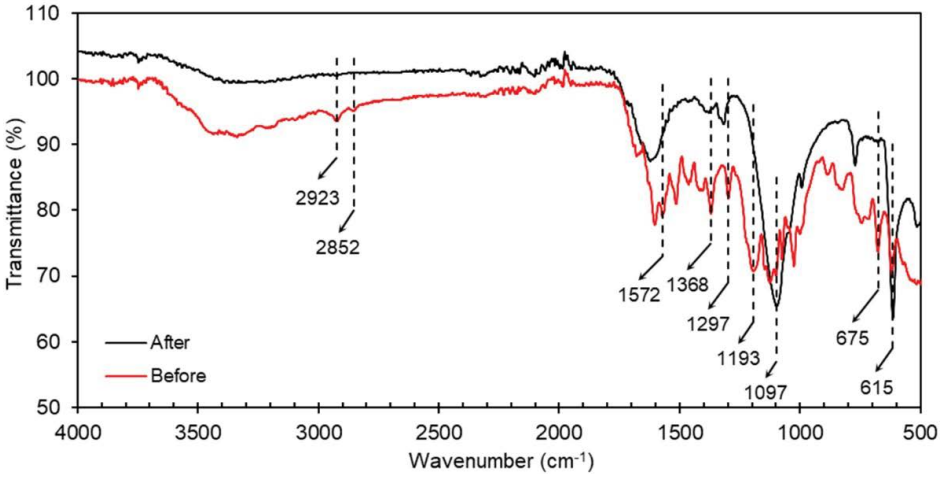

Fig. 8. FTIR spectra before and after treatment for dye material.

ion presence. Additionally, initial DOHF concentration causes a reduction in the decolorization rate. Experimental kinetic data under different reaction conditions showed that the DOHF decolorization kinetics closely followed BMG kinetics. Finally, FTIR results confirmed that major structure of dye molecule was destructured. After determining proper doses of the experimental parameters, Fenton oxidation process can also be used for the decolorization of different dyes from industrial wastewaters.

Acknowledgments

This study was completed in Kastamonu University Central Research Laboratory and was supported by Kastamonu University Scientific Research Projects Management Coordination Unit (Grant No: KÜ-BAP01/2016-32).

References

[1] X. Shi, A. Tian, J. You, H. Yang, Y. Wang, X. Xue, Degradation of organic dyes by a new heterogeneous Fenton reagent - Fe_2GeS_4 nanoparticle, J. Hazard. Mater., 353 (2018) 182–189.
[2] P.V. Nidheesh, M. Zhou, M.A. Oturan, An overview on the removal of synthetic dyes from water by electrochemical advanced oxidation processes, Chemosphere, 197 (2018) 210–227.
[3] P.A. Carneiro, R.F.P. Nogueira, M.V.B. Zanoni, Homogeneous photodegradation of C.I. Reactive Blue 4 using a photo-Fenton process under artificial and solar irradiation, Dyes Pigm., 74 (2006) 127–132.
[4] Y.L. Pang, A.Z. Abdullah, S. Bhatia, Review on sonochemical methods in the presence of catalysts and chemical additives for treatment of organic pollutants in wastewater, Desalination, 277 (2011) 1–14.
[5] S. Papić, D. Vujević, N. Koprivanac, D. Šinko, Decolourization and mineralization of commercial reactive dyes by using homogeneous and heterogeneous Fenton and UV/Fenton processes, J. Hazard. Mater., 164 (2009) 1137–1145.
[6] A. Hassani, C. Karaca, S. Karaca, A. Khataee, Ö. Açışlı, B. Yılmaz, Enhanced removal of basic violet 10 by heterogeneous sono-Fenton process using magnetite nanoparticles, Ultrason. Sonochem., 42 (2018) 390–402.
[7] M. Muruganandham, M. Swaminathan, Photocatalytic decolourisation and degradation of Reactive Orange 4 by TiO_2-UV process, Dyes Pigm., 68 (2006) 133–142.
[8] F. Rehman, M. Sayed, J.A. Khan, N.S. Shah, H.M. Khan, D.D. Dionysiou, Oxidative removal of brilliant green by UV/$S_2O_8^{2-}$, UV/HSO_5^- and UV/H_2O_2 processes in aqueous media: a comparative study, J. Hazard. Mater., 357 (2018) 506–514.
[9] J. Wang, Y. Jiang, Z. Zhang, X. Zhang, T. Ma, G. Zhang, G. Zhao, P. Zhang, Y. Li, Investigation on the sonocatalytic degradation of acid red B in the presence of nanometer TiO_2 catalysts and comparison of catalytic activities of anatase and rutile TiO_2 powders, Ultrason. Sonochem., 14 (2007) 545–551.
[10] H. Hayat, Q. Mahmood, A. Pervez, Z.A. Bhatti, S.A. Baig, Comparative decolorization of dyes in textile wastewater using biological and chemical treatment, Sep. Purif. Technol., 154 (2015) 149–153.
[11] Q.H. Hu, S.Z. Qiao, F. Haghseresht, M.A. Wilson, G.Q. Lu, Adsorption study for removal of basic red dye using bentonite, Ind. Eng. Chem. Res., 45 (2006) 733–738.
[12] W. Bae, H. Won, B. Hwang, R.A. de Toledo, J. Chung, K. Kwon, H. Shim, Characterization of refractory matters in dyeing wastewater during a full-scale Fenton process following pure-oxygen activated sludge treatment, J. Hazard. Mater., 287 (2015) 421–428.
[13] S. Şahinkaya, COD and color removal from synthetic textile wastewater by ultrasound assisted electro-Fenton oxidation process, J. Ind. Eng. Chem., 19 (2013) 601–605.
[14] Y.K. Bayhan, G.D. Değermenci, Investigation of kinetic and removal of organic matter from cosmetic wastewaters by fenton process, J. Faculty Eng. Archit. Gazi Univ., 32 (2017) 203–210.
[15] L.C. Chavaco, C.A. Arcos, D. Prato-Garcia, Decolorization of reactive dyes in solar pond reactors: perspectives and challenges for the textile industry, J. Environ. Manage., 198 (2017) 203–212.
[16] C. Özdemir, H. Tezcan, S. Sahinkaya, E. Kalipci, Pretreatment of olive oil mill wastewater by two different applications of Fenton oxidation processes, Clean Soil Air Water, 38 (2010) 1152–1158.
[17] R. Li, C. Yang, H. Chen, G. Zeng, G. Yu, J. Guo, Removal of triazophos pesticide from wastewater with Fenton reagent, J. Hazard. Mater., 167 (2009) 1028–1032.
[18] Ö. Gökkuş, F. Çoşkun, M. Kocaoğlu, Y.Ş. Yıldız, Determination of optimum conditions for color and COD removal of Reactive Blue 19 by Fenton oxidation process, Desal. Wat. Treat., 52 (2014) 6156–6165.
[19] M.A. Behnajady, N. Modirshahla, F. Ghanbary, A kinetic model for the decolorization of C.I. Acid Yellow 23 by Fenton process, J. Hazard. Mater., 148 (2007) 98–102.
[20] M.S. Lucas, J.A. Peres, Decolorization of the azo dye Reactive Black 5 by Fenton and photo-Fenton oxidation, Dyes Pigm., 71 (2006) 236–244.

[21] M. Radwan, M. Gar Alalm, H. Eletriby, Optimization and modeling of electro-Fenton process for treatment of phenolic wastewater using nickel and sacrificial stainless steel anodes, J. Water Process Eng., 22 (2018) 155–162.
[22] I. Michael, E. Hapeshi, C. Michael, D. Fatta-Kassinos, Solar Fenton and solar TiO_2 catalytic treatment of ofloxacin in secondary treated effluents: evaluation of operational and kinetic parameters, Water Res., 44 (2010) 5450–5462.
[23] A. Tabasum, M. Zahid, H.N. Bhatti, M. Asghar, Fe_3O_4-GO composite as efficient heterogeneous photo-Fenton's catalyst to degrade pesticides, Mater. Res. Express. 6 (2019) 015608.
[24] J. Khan, M. Sayed, F. Ali, H.M. Khan, Removal of Acid Yellow 17 Dye by Fenton Oxidation Process, Zeitschrift Fur Phys. Chemie., 232 (2018) 507–525.
[25] J.H. Sun, S.P. Sun, G.L. Wang, L.P. Qiao, Degradation of azo dye Amido black 10B in aqueous solution by Fenton oxidation process, Dyes Pigm., 74 (2007) 647–652.
[26] S.P. Sun, C.J. Li, J.H. Sun, S.H. Shi, M.H. Fan, Q. Zhou, Decolorization of an azo dye Orange G in aqueous solution by Fenton oxidation process: effect of system parameters and kinetic study, J. Hazard. Mater., 161 (2009) 1052–1057.
[27] V. Kavitha, K. Palanivelu, Destruction of cresols by Fenton oxidation process, Water Res., 39 (2005) 3062–3072.
[28] P. Bautista, A.F. Mohedano, M.A. Gilarranz, J.A. Casas, J.J. Rodriguez, Application of Fenton oxidation to cosmetic wastewaters treatment, J. Hazard. Mater., 143 (2007) 128–134.
[29] A. Babuponnusami, K. Muthukumar, A review on Fenton and improvements to the Fenton process for wastewater treatment, J. Environ. Chem. Eng., 2 (2014) 557–572.
[30] M.G. Alalm, A. Tawfik, S. Ookawara, Degradation of four pharmaceuticals by solar photo-Fenton process: kinetics and costs estimation, J. Environ. Chem. Eng., 3 (2015) 46–51.
[31] S.H. Lin, C.C. Lo, Fenton process for treatment of desizing wastewater, Water Res., 31 (1997) 2050–2056.
[32] S.H. Lin, chi M. Lin, H.G. Leu, Operating characteristics and kinetic studies of surfactant wastewater treatment by fenton oxidation, Water Res., 33 (1999) 1735–1741.
[33] M.W. Chang, J.M. Chern, Decolorization of peach red azo dye, HF6 by Fenton reaction: Initial rate analysis, J. Taiwan Inst. Chem. Eng., 41 (2010) 221–228.
[34] H. Titouhi, J.E. Belgaied, Heterogeneous Fenton oxidation of ofloxacin drug by iron alginate support, Environ. Technol. (United Kingdom), 37 (2016) 2003–2015.
[35] H. Li, Y. Li, L. Xiang, Q. Huang, J. Qiu, H. Zhang, M.V. Sivaiah, F. Baron, J. Barrault, S. Petit, S. Valange, Heterogeneous photo-Fenton decolorization of Orange II over Al-pillared Fe-smectite: Response surface approach, degradation pathway, and toxicity evaluation, J. Hazard. Mater., 287 (2015) 32–41.
[36] A. Mirzaei, Z. Chen, F. Haghighat, L. Yerushalmi, Removal of pharmaceuticals from water by homo/heterogonous Fenton-type processes – a review, Chemosphere, 174 (2017) 665–688.
[37] N.U.H. Khan, H.N. Bhatti, M. Iqbal, A. Nazir, Decolorization of basic turquise blue X-GB and basic blue X-GRRL by the Fenton's process and its kinetics, Zeitschrift Fur Phys. Chemie., 233 (2019) 361–373.
[38] M.V. Bagal, P.R. Gogate, Wastewater treatment using hybrid treatment schemes based on cavitation and Fenton chemistry: a review, Ultrason. Sonochem., 21 (2014) 1–14.
[39] M. Sayed, A. Arooj, N.S. Shah, J.A. Khan, L.A. Shah, F. Rehman, H. Arandiyan, A.M. Khan, A.R. Khan, Narrowing the band gap of TiO_2 by co-doping with Mn^{2+} and Co^{2+} for efficient photocatalytic degradation of enoxacin and its additional peroxidase like activity: a mechanistic approach, J. Mol. Liq., 272 (2018) 403–412.
[40] N.S. Shah, J.A. Khan, M. Sayed, Z.U.H. Khan, A.D. Rizwan, N. Muhammad, G. Boczkaj, B. Murtaza, M. Imran, H.M. Khan, G. Zaman, Solar light driven degradation of norfloxacin using as-synthesized Bi^{3+} and Fe^{2+} co-doped ZnO with the addition of HSO_5^-: toxicities and degradation pathways investigation, Chem. Eng. J., 351 (2018) 841–855.
[41] N.S. Shah, J.A. Khan, M. Sayed, Z.U.H. Khan, H.S. Ali, B. Murtaza, H.M. Khan, M. Imran, N. Muhammad, Hydroxyl and sulfate radical mediated degradation of ciprofloxacin using nano zerovalent manganese catalyzed $S_2O_8^{2-}$, Chem. Eng. J., 356 (2019) 199–209.
[42] S.S. Ashraf, M.A. Rauf, S. Alhadrami, Degradation of Methyl Red using Fenton's reagent and the effect of various salts, Dyes Pigm., 69 (2006) 74–78.
[43] C. Sirtori, A. Zapata, I. Oller, W. Gernjak, A. Agüera, S. Malato, Solar photo-fenton as finishing step for biological treatment of a pharmaceutical wastewater, Environ. Sci. Technol., 43 (2009) 1185–1191.
[44] F. Emami, A.R. Tehrani-Bagha, K. Gharanjig, F.M. Menger, Kinetic study of the factors controlling Fenton-promoted destruction of a non-biodegradable dye, Desalination, 257 (2010) 124–128.
[45] S. Tunç, O. Duman, T. Gürkan, Monitoring the decolorization of acid orange 8 and acid red 44 from aqueous solution using Fenton's reagents by online spectrophotometric method: effect of operation parameters and kinetic study, Ind. Eng. Chem. Res., 52 (2013) 1414–1425.
[46] S. Raghu, C.W. Lee, S. Chellammal, S. Palanichamy, C.A. Basha, Evaluation of electrochemical oxidation techniques for degradation of dye effluents-A comparative approach, J. Hazard. Mater., 171 (2009) 748–754.
[47] J. Wei, Y. Song, X. Tu, L. Zhao, E. Zhi, Pretreatment of dry-spun acrylic fiber manufacturing wastewater by Fenton process: optimization, kinetics and mechanisms, Chem. Eng. J., 218 (2013) 319–326.
[48] J. Wei, Y. Song, X. Meng, X. Tu, J.-S. Pic, Transformation characteristics of organic pollutants in Fered-Fenton process for dry-spun acrylic fiber wastewater treatment, Water Sci. Technol., 70 (2014) 1976–1982.
[49] D. Ami, P. Mereghetti, M. Leri, S. Giorgetti, A. Natalello, S.M. Doglia, M. Stefani, M. Bucciantini, A FTIR microspectroscopy study of the structural and biochemical perturbations induced by natively folded and aggregated transthyretin in HL-1 cardiomyocytes, Sci. Rep., 8 (2018) 12508.
[50] D.C. Kalyani, A.A. Telke, R.S. Dhanve, J.P. Jadhav, Ecofriendly biodegradation and detoxification of Reactive Red 2 textile dye by newly isolated *Pseudomonas* sp. SUK1, J. Hazard. Mater., 163 (2009) 735–742.
[51] A. Fahmy, A. El-Zomrawy, A.M. Saeed, A.Z. Sayed, M.A. Ezz El-Arab, H.A. Shehata, Modeling and optimizing Acid Orange 142 degradation in aqueous solution by non-thermal plasma, Chemosphere, 210 (2018) 102–109.
[52] L. Pereira, P.K. Mondal, M. Alves, Aromatic Amines Sources, Environmental Impact and Remediation, Springer, Cham, 2015, pp. 297–346.
[53] D.R. Patel, B.M. Patel, N.B. Patel, K.C. Patel, Application of newly synthesized bisazo dichloro-s-triazinyl reactive dyes bearing 1,3,4-oxadiazole molecule, J. Saudi Chem. Soc., 18 (2014) 245–254.
[54] M. Ursescu, T. Măluţan, S. Ciovicˇ, Iron gall inks influence on papers' thermal degradation FTIR spectroscopy applications, Eur. J. Sci. Theol., 5 (2009) 71–84.
[55] K. Nakamoto, Infrared and Raman Spectra of Inorganic and Coordination Compounds, Theory and Applications in Inorganic Chemistry, 6th ed., Wiley, New Jersey, 2009.